Changes in geothermal reservoirs due to hydrothermal eruptions and fault reactivation

James Patterson[1], Mark P. Simpson[1]

[1]GNS Science, Wairakei Research Centre, 114 Karetoto Road, RD4, Taupo 3384, New Zealand

j.patterson@gns.cri.nz

Keywords: *Geothermal Reservoir, Reservoir Modelling, Hydrothermal Eruption, Fault*

ABSTRACT

Geothermal reservoirs naturally change over time as hot upflows shift within the subsurface. The causes of such evolving flow paths are often speculated upon. Of the many possible mechanisms, large hydrothermal eruptions (focal depth > 100 m) and faulting (new or reactivation) may cause sudden changes in the pressure and flow field locally, leading to changes in temperature and pressure in the deeper subsurface. The extent and magnitude of such changes are poorly understood.

We employ a numerical reservoir simulator to investigate how fluid flow throughout the geothermal system is affected by a sizable hydrothermal eruption or permeable fault zone. By using simplified models, we identify scenarios in which these mechanisms have greatest impact and set bounds on the extent and magnitude of change. We show that the permeable zone created by a hydrothermal eruption has strong impacts on the pressure, temperature, and flow regime in the shallow reservoir (<1 km), but their effect on the deeper reservoir (>1 km) can be limited in the presence of deeper flow barriers (i.e., a deep clay cap). By contrast, fault development extending into the deeper reservoir and penetrating such flow barriers has the capacity to alter the system by slightly shifting where hot upflows move into the shallow system. Our findings can be applied to other reservoirs, providing a first-order assessment of whether hydrothermal eruptions and/or faulting could be responsible for the changes in the temperature, pressure, and hydrologic structure of the geothermal system.

1. INTRODUCTION

Geothermal systems are highly dynamic and change with time. Typical changes include natural thermal decline via cooling of the heat source, mineral sealing via alteration/deposition, and incursion of cooler fluids. But more dramatic changes can include geothermal disruption by volcanic or tectonic events, faulting, or by a sizable hydrothermal eruption or eruptions. These events have all been identified as drivers of change in geothermal systems of the Taupō Volcanic Zone (TVZ) of Aotearoa, New Zealand.

While these events profoundly affect the thermal and hydrological structure of geothermal system (Simpson et al. 2021), the full extent and progression of change over time is less well known. To gain better insight, we model the effects of a hydrothermal eruption and separately fault activation on a theoretical geothermal system and investigate the effects on the fluid flow. We employ a numerical reservoir simulator to determine how a hydrothermal eruption may disrupt shallow or deep reservoirs, then look at how a permeable fault may disrupt the reservoirs. Furthermore, for these two scenarios we investigate several simulations by varying the permeability and the locations of a hydrothermal eruption vent centre or fault within the geothermal system.

2. GEOTHERMAL SYSTEM CHANGE

In the TVZ the hydrologic and thermal setting of several geothermal systems have changed with time. Here we highlight three examples. The hydrological/thermal structure of the Waimangu-Rotomahana geothermal system was modified by the 1886 Mount Tarawera eruption (Simmons & O'Sullivan 2010). A 16 km rift zone cuts through Mount Tarawera and its extension through ancestral Lake Rotomahana and Waimangu Valley is represented by several structurally aligned magmatic-hydrothermal and hydrothermal eruption centres attributed to dyke intrusion. New fluid pathways created though the Waimangu Valley resulted in the appearance of thermal features where previously there were none (Simmons et al., 1993). Bubble plumes and high heat flux in Lake Rotomahana beyond the well-defined demagnetised zone suggest post-eruption extension of geothermal activity in this area (Tontini et al., 2015). Thus the 1886 eruption resulted in new breccia and structurally controlled fluid pathways through the existing geothermal system.

At Te Kopia, movement along the Paeroa Fault has disrupted the geothermal system as revealed from hydrothermal minerals and fluid inclusions (Bignall and Browne, 1994). In the exposed fault scarp acid minerals from steam condensates (kaolinite ± alunite ± sulfur) overprint earlier adularia and illite that formed from chloride waters at >220°C and ≥250 m below the water table. Fluid inclusions in quartz crystals are also estimated to have formed at least 230 m below the water table (Bignall et al., 2004). Complex crystal growth seen from SEM cathodoluminescence imaging is interpreted to reflect repeated movement on the Paeroa Fault (Bignall et al., 2004). Geothermal activity has continued post-faulting with juxtaposition of acid next to neutral alteration minerals in the upthrown block.

At Rotokawa the geothermal system has been disrupted by inferred fault activity and further by multiple sizable hydrothermal eruptions (Simpson et al., 2021; Montanaro et al., 2023). Epidote and fluid inclusions reveal past hot conditions in the northern extent of the field (hotter by up to 50°C), whereas the main upflow and hottest fluids presently occur towards the south. Alteration intensity is greater to the north, suggesting past greater water-rock interaction than in the south. It is postulated reactivation of the Central Field Fault (several faults and damage zones) has shifted the focus of upflow to the south with reduced flow to the north (Simpson et al., 2021). In addition, there have been at least eight large hydrothermal eruptions in the southern portion of the field with vent centres extending over 1.7 km broadly aligned with the Central Field Fault (Collar and Browne, 1985; Montanaro et al., 2023). The largest breccia deposit covers an area ~4 km in diameter and ejected breccia sourced from ~275 m and possibly up to ~450 m depth (Collar and

ISSN 2703-4275

Browne, 1985). The impact of these eruptions is inferred from mineralogy. Eruption induced pressure drawdown is interpreted to have resulted in the deposition of anhydrite to ~500 m depth and eruption induced transient decompressive boiling considered responsible for widespread chalcedony at >1,200 m depth. At Rotokawa, faulting and hydrothermal eruptions have changed both the deep and shallow hydrologic and thermal construct of the geothermal system, respectively.

3. METHODOLOGY AND MODEL SETUP

Numerical simulations investigating the impact of a hydrothermal eruption or a fault on the permeability of a geothermal system were carried out using TOUGH2, the standard reservoir simulator used by the geothermal industry (Pruess 1999, Burnell et al. 2012). A 2D model is set up, with a horizontal length of 10 km and a vertical depth of 5 km from surface to the bottom of the domain, discretised using a refined grid comprised of 41,180 cells. Cells near the eruption or fault zones are 10 m wide; further away at the edges of the domain the cells are 50 m wide. The topography was modelled as flat, as the focus of this work is to understand how hydrothermal eruptions and faults may change the flow and temperature fields in a generic geothermal reservoir. The model used EOS 1 with no-flow boundary conditions at the sides and bottom and an open atmosphere cell at the top, where rainfall was allowed to enter the model.

The model consists of a shallow reservoir from 0 to 1 km depth and a deep reservoir from 1 to 5 km depth. A shallow clay cap exists from 100 to 200 m and a deep clay cap exists from 800 to 1000 m depth separating the shallow and deep reservoirs. This structure and temperatures broadly matches several TVZ geothermal systems, loosely paralleling that for the Rotokawa (Winick et al., 2011; Sewell et al. 2015), and Nga Tamariki geothermal fields (O'Brien et al. 2011; Chambefort et al. 2016), that have a main reservoir at >1km depth with both shallow and deep clay caps.

Rock properties and other model parameters are given in Table 1. Rock properties other than permeability are generalised and similar for all rock types in the model. Figure 1 shows a sample layout of the model domain. Some features of the model, such as the location of the eruption and fault zone, are changed in different simulations and will therefore deviate from the figure. The permeability of the deep clay cap was also varied in the models.

Simulations are run for 30,000 years, reaching a kind of natural state (though not steady state) before either a hydrothermal eruption or fault zone is introduced. There is no history matching performed, as this is a simplified theoretical model. In nature, hydrothermal eruptions are understood to occur in places where the fluids are near boiling and the eruption triggered by sudden decompression (Browne and Lawless, 2001). As pressure is released and fluids instantaneously boils (flashes) and this further reduces pressure with the boiling front propagating downwards and material being ejected till explosive energy is no longer sufficient to excavate. The explosive release results in the ejection of steam and rock and breccia deposits around the eruption vent. Simulating the eruption and immediate associated changes is outside the scope of this work. Here, we model the long term (>1,000 years) remnant of a hydrothermal eruption as a region of higher permeability (i.e. more permeable than the host rock) providing a conduit between the geothermal system and the surface. In the TOUGH2 model, the eruption vent / zone scenario is modelled as 100 m wide and 200 m deep, penetrating a shallow clay cap (100 to 200 m below surface).

In the fault scenario, the fault zone is modelled as a zone of increased permeability extending from surface to 2000 m depth. Fault zones are important reservoir features where host matrix permeabilities are often too low to facilitate convective flows. Many fault zones exhibit only temporary permeability, as mineral precipitation or other mechanisms may close those fluid pathways on the order of thousands of years (Dempsey et al. 2012), but in this work, we assume the fault zone remains permeable.

After the placement of an eruption or fault zone in the model, the simulation resumes and is run for an additional 5,000 years post natural state. An alternate base-case model undisrupted by a hydrothermal eruption or fault is also run for an additional 5,000 years post natural state, allowing for the direct comparison with the eruption and fault simulation. Both the hydrothermal eruption and fault zone have been modelled to remain permeable for the duration of the simulation.

Model parameters are varied to investigate their effects on the resultant temperature changes: time since placement of the permeable zone (500 to 5,000 years), eruption/fault zone permeability (1e-16 m^2 to 1e-13 m^2), deep clay cap permeability (1e-19 m^2 to 1e-16 m^2), and placement of the eruption/fault zone (offset from centre-line of -2,000 to +2,000 m).

Table 1: Boundary conditions and rock properties.

Boundary Conditions	
Surface pressure	0.1 MPa
Surface temperature	10 °C
Basal heat flow	0.1 W/m^2
Hot water inflow	10 kg/s @ 350 °C
Rock Properties (all rock types)	
Rock Density	2500 kg/m^3
Heat capacity	800 kJ/kg
Porosity	0.08
Thermal conductivity	2.0 W/mK
Rock Permeabilities	
Reservoir permeability (high)	1e-15 m^2
Reservoir permeability (low)	1e-17 m^2
Clay permeability	1e-19 m^2
Shallow sediment permeability	1e-15 m^2
Eruption zone permeability	1e-14 m^2
Fault zone permeability	1e-14 m^2

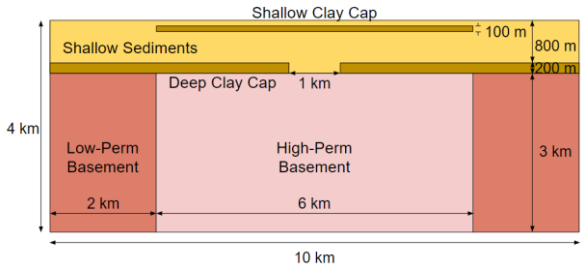

Figure 1: Generalised model setup used for all simulations. Location of permeable gap in deep clay layer varies between models.

ISSN 2703-4275

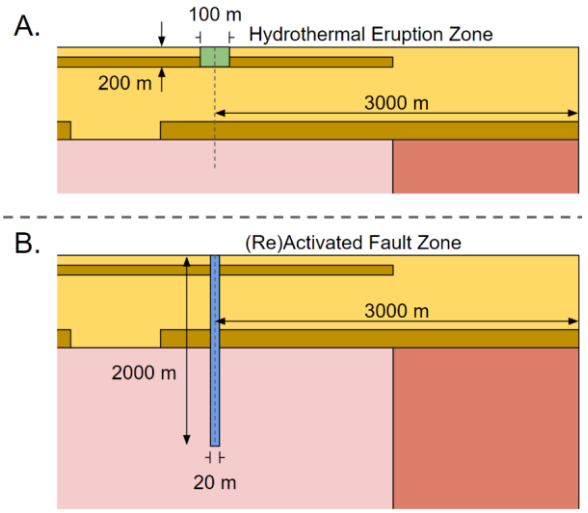

Figure 2: Two generalised model setups: A) with hydrothermal eruption zone and B) with fault zone. Location of these zones varies between models. Eruption zone and fault zone not drawn to scale.

4. RESULTS

The presence of a hydrothermal eruption or fault zone induces temperature changes compared to the base-case: some areas become warmer, while others become cooler. We use the term "heating" and "cooling" to refer to the difference in temperature between the eruption/fault model and the base-case model.

4.1 HYDROTHERMAL ERUPTION

When the shallow clay cap is pierced by a hydrothermal eruption, fluid quickly flows upward, as hydrothermal eruptions occur only where the underlying reservoir is near boiling with significant buoyant force. As fluid boils and moves towards the surface, reservoir pressure drops and draws in fluid from the surrounding area. This causes upwelling fluid to preferentially flow towards the eruption zone, starving adjacent areas of hot water which in turn cool over time. Figure 3 shows the reservoir's temperature field 5,000 years after a hydrothermal eruption zone, along with the temperature difference calculated against a model without an eruption zone. The eruption zone is seen as a small area of elevated temperature near the top of the model.

Figure 4 shows temperature changes at different times following a hydrothermal eruption. Temperature changes occur rapidly, but plateau quickly and take time to spread to other parts of the reservoir. Within 500 years, reservoir temperatures increase by up to +57 °C. A temperature change of +20 °C extends down to 400 m below surface (i.e., 200 m below the bottom of the eruption zone) and up to 250 m away from the eruption zone. Minor cooling, around -5 °C occurs in small, isolated regions away from the eruption zone.

At 5,000 years, the maximum heating reaches +113 °C with the +20 °C zone extending to 425 m below surface and up to 950 m laterally from the eruption zone. The maximum cooling effect observed reaches -116 °C at a location 175 m below the surface and nearly 1800 m away from the eruption centre. For both heating and cooling, the temperature change is mostly confined between the two low-permeability clay caps, within 800 m of the surface. Below 1000 m depth the maximum temperature increase and decrease are +1 °C and -24 °C, respectively. Thus, though the heating effect is stronger in the shallow reservoir above 1000 m, the cooling effect is greater below 500 m, both in terms of magnitude and extent. Below 1550 m, the reservoir temperature does not change more than ±5 °C.

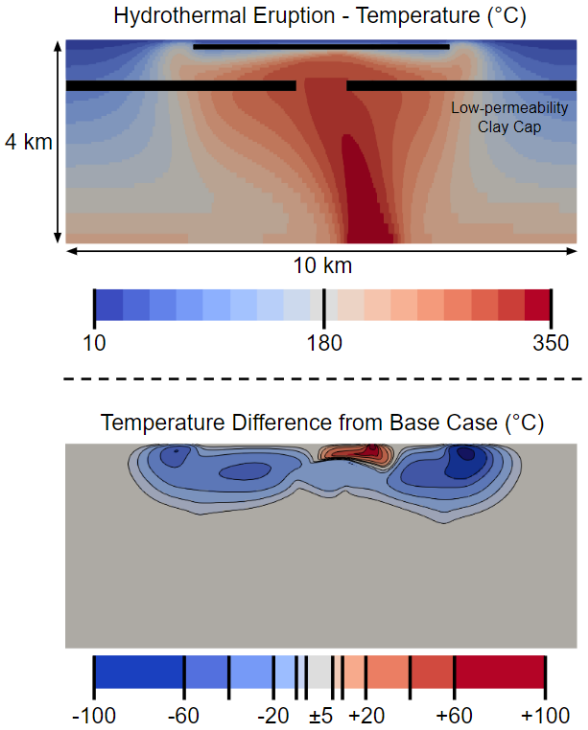

Figure 3: Reservoir temperature and change in temperature due to a hydrothermal eruption after 5,000 years. Model properties are given in Table 1. In the image showing temperature (above), each discrete colour represents a band of 20 °C. In the image showing temperature difference (below), colours and contours are set at ±5, ±10, ±20, ±40, ±60, and ±100 °C. Grey represents a temperature difference of less than ±5 °C.

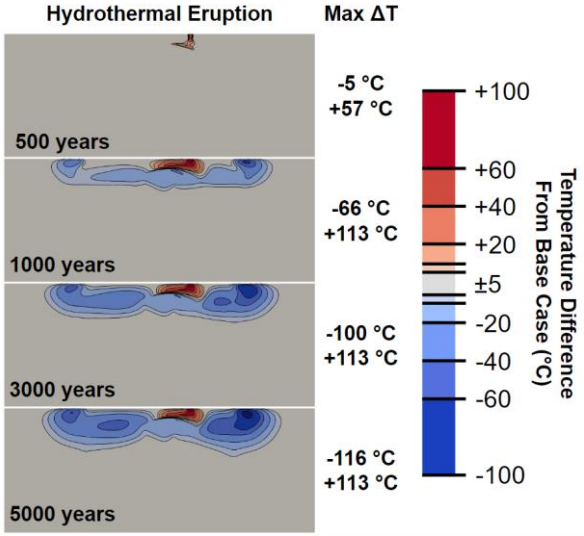

Figure 4: Change in reservoir temperature due to a hydrothermal eruption at time intervals of 500, 1,000, 3,000, and 5,000 years after formation of the eruption zone. Colours and contours are set at ±5, ±10, ±20, ±40,

ISSN 2703-4275

±60, and ±100 °C. Grey represents a temperature difference of less than ±5 °C.

Simulations investigating different permeabilities of the eruption zone (10^{-16} to 10^{-13} m^2) have been run based on estimates of hydrothermal eruptions by Heap et al. (2017). The permeability of the reservoir and shallow permeable units was set at 10^{-15} m^2, and of the clay cap at 10^{-19} m^2. Figure 5 shows the temperature difference of these models after 5,000 years of simulation time. At low eruption permeabilities, temperature increases are significantly stronger than temperature decreases, as relatively little hot fluid flows upwards through the eruption zone rather than laterally. As permeability increases, the heating effect around the eruption zone appears to plateau, as water reaches the boiling point temperature. Meanwhile, the distal cooling effect strengthens as hot fluid preferentially flows through the eruption zone rather than other portions of the reservoir.

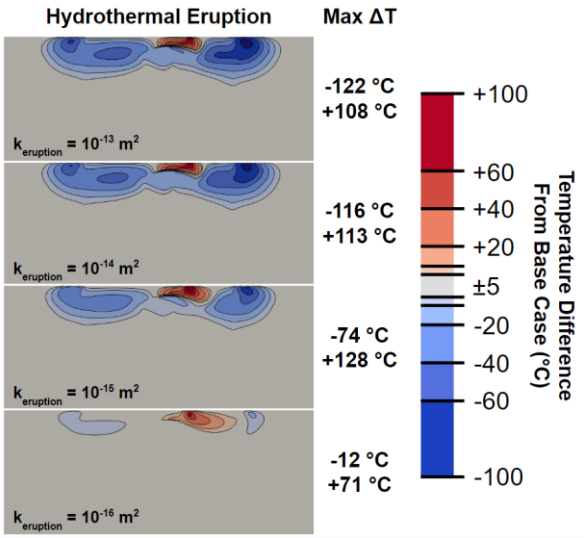

Figure 5: Change in reservoir temperature due to a hydrothermal eruption with varying eruption zone permeability. Eruption zone permeability is set to 1E-13 m^2, 1E-14 m^2, 1E-15 m^2, and 1E-16 m^2. Colours and contours are set at ±5, ±10, ±20, ±40, ±60, and ±100 °C. Grey represents a temperature difference of less than ±5 °C.

Figure 6 shows different scenarios in which the deep clay cap permeability is varied from 1E-19 m^2 to 1E-15 m^2 while eruption zone permeability is constant at 1E-14 m^2. As clay cap permeability increases, fluid is better able to circulate from the deep upflow to shallow depths. This upward flowing hot fluid is no longer constrained to flow through the hole in the clay cap, which is a 1000 m wide permeable region in the centreline of the model from 800 m to 1000 m depth. This alters the overall convection pattern within the reservoir, changing it from that seen in Figure 3.

When the permeability of the cap is increased, the magnitude of heating increases and the heating effect is observed over a greater area, both laterally and vertically. Conversely, the magnitude and lateral extent of the cooling effect decreases, though the vertical extent of cooling increases slightly. Without the deep clay cap creating a tortuous flow path for upwelling fluids, convective patterns at depth are more susceptible to changes induced by the hydrothermal eruption near the surface.

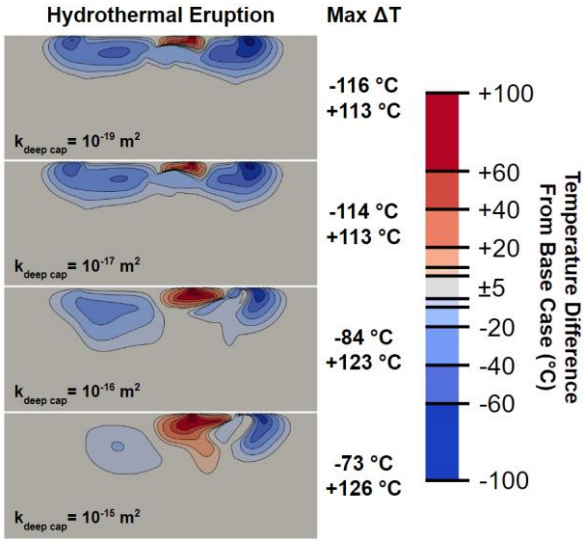

Figure 6: Change in reservoir temperature in response to a hydrothermal eruption in a system with varying deep clay cap permeability at 10,000 years. Deep clay cap permeability is set to 1E-19 m^2, 1E-17 m^2, 1E-16 m^2 , and 1E-15 m^2. Colours and contours are set at ±5, ±10, ±20, ±40, ±60, and ±100 °C. Grey represents a temperature difference of less than ±5 °C.

The location of the hydrothermal eruption zone with respect to the hole in the deeper clay cap plays a negligible role in the magnitude and location of thermal changes. The location of a hydrothermal eruption is constrained to those areas where temperatures below the shallow clay cap are near boiling, which encompasses a relatively small area in this model. Simulations in which the eruption zone location is varied result in temperature differences similar to those observed in Figure 4 and are therefore not shown here.

4.2 Fault Zone

The sudden appearance of a high-permeability fault zone in the reservoir system has an effect similar to that of a hydrothermal eruption, but with two key differences. Firstly, a fault zone can extend deeper than a hydrothermal eruption, piercing the deep clay cap. Secondly, a fault zone can propagate through any part of the geothermal system, including regions where the reservoir temperatures are significantly below boiling.

Figure 7 shows how reservoir temperature changes after the appearance of a permeable fault zone, extending from surface to 2000 m depth. Similar to the temperature changes induced by a hydrothermal eruption, the rock in the immediate vicinity of a permeable fault quickly heats up, as hot fluid from below rises towards the surface. However, the magnitude of the heating is significantly stronger, up to +108 °C after only 500 years.

The cooling effect at 500 years is relatively minor, up to -4 °C. After 5,000 years, the maximum temperature change observed is +130 °C and -86 °C, indicating that the heating effect is both stronger and quicker to appear. Again, this is due to hot fluids quickly flowing into cool host rock above, immediately heating the surrounding rock. With this new flow path, the hot fluid no longer flows to other parts of the reservoir, causing those regions to slowly cool down as heat diffuses away.

The extent of the temperature change varies greatly between heating and cooling. The zone of heating forms quickly but is

ISSN 2703-4275

relatively shallow: a temperature increase of +10 °C extends down to 475 m below surface after only 500 years, then down to 1350 m after 5,000 years. The zone of cooling, however, forms slowly and covers a wide area. No cooling is observed after 500 years, but after 5,000 years a region of cooling of -10 °C extends down to the bottom of the model at 4000 m depth.

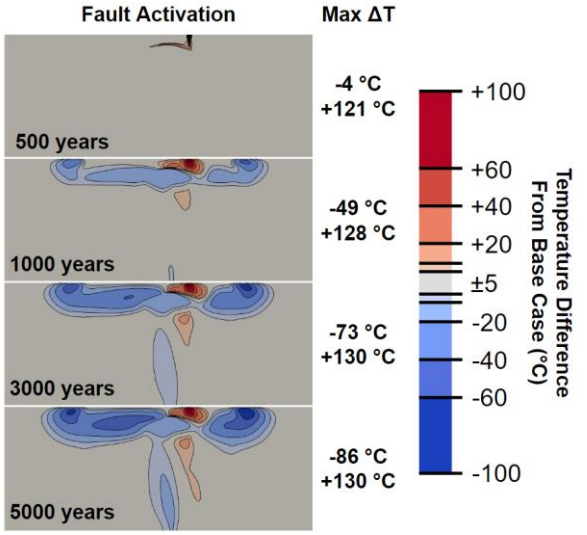

Figure 7: Change in reservoir temperature due to fault activation or reactivation at time intervals of 500, 1,000, 3,000, and 5,000 years after formation of the fault zone. Colours and contours are set at ±5, ±10, ±20, ±40, ±60, and ±100 °C. Grey represents a temperature difference of less than ±5 °C.

As modelled for the eruption zones, we have varied the permeability of the fault zone from highly permeable (1E-13 m^2) to an order of magnitude less than that of the reservoir rock (1E-16 m^2), with the results shown in Figure 9 after 5,000 years. At a fault permeability of 1E-16 m^2, only minor temperature changes are observed. Just one order of magnitude higher at 1E-15 m^2, a temperature increase of +120 °C is observed. Anther order of magnitude increase to 1E-14 m^2, yields similar heating effects, indicating that there is a kind of "critical" permeability above which a fault begins to strongly affect the temperature field of the reservoir. The area over which this temperature change occurs varies laterally and vertically, but remains focussed in a relatively small area.

In contrast, the cooling effect from fault permeabilities intensifies gradually from -4 °C (1E-16 m^2) to -25 °C (1E-15 m^2), then -86 °C (1E-14 m^2), and finally -141 °C (1E-13 m^2). As fault permeability increases, the lateral and vertical extent of this cooling also intensifies.

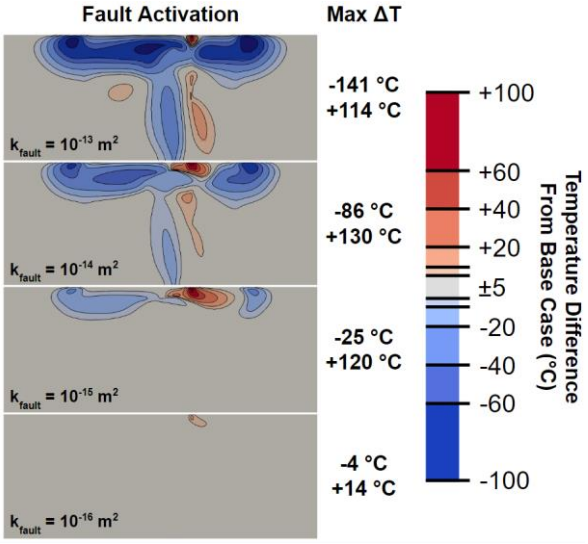

Figure 8: Change in reservoir temperature due to a fault zone with varying permeability. Fault zone permeability is set to 1E-16 m^2, 1E-15 m^2, 1E-14 m^2, and 1E-13 m^2. Colours and contours are set at ±5, ±10, ±20, ±40, ±60, and ±100 °C. Grey represents a temperature difference of less than ±5 °C.

As modelled for the eruption zones, we varied the deep clay cap permeability from relatively impermeable (1E-19 m^2) to that of the reservoir rock (1E-15 m^2; Figure 9). As clay cap permeability increases, the lateral extent of the temperature change becomes vertically more confined to shallow depths and laterally more confined to the area around the fault zone. This is similar to the pattern observed in the eruption zone results (Figure 6).

The high-permeability fault zone focuses this upflow and allows it to flow to the surface more quickly than through the background reservoir rock. This causes the shallow system to heat up, while the regions adjacent to the original upflow receive less hot water. Between the models shown in Figure 9, the regions of cooling are spatially distributed differently, due to differing initial convection patterns. As clay cap permeability increases, the magnitude of heating remains within +130 and +138 °C, while the magnitude of cooling decreases from -87 to -60 °C.

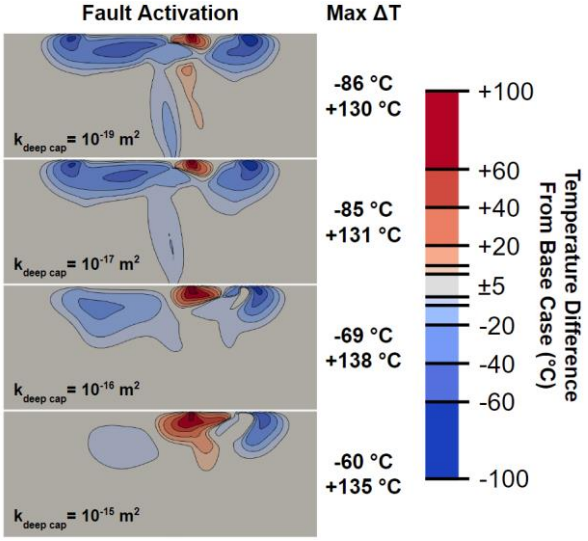

ISSN 2703-4275

Figure 9: Change in reservoir temperature in response to a hydrothermal eruption in a system with varying deep clay cap permeability at 10,000 years. Deep clay cap permeability is set to 1E-13 m^2, 1E-14 m^2, 1E-15 m^2, and 1E-16 m^2. Colours and contours are set at ±5, ±10, ±20, ±40, ±60, and ±100 °C. Grey represents a temperature difference of less than ±5 °C.

Since the location of the fault is unrestricted, it can occur away from region of high temperature beneath the clay cap. Figure 10 shows simulations in which the fault zone is offset from the hole in the deeper clay cap. The spacing interval between figures is 1000 m. In all cases, the permeable fault acts as a conduit for deep, hot fluid to flow across the shallow clay cap. However, when offset -2000 m from the midline (i.e., towards the left), the fault penetrates the reservoir in a relatively cool region where fluid was flowing downward.

Therefore, below the deep clay cap, in this scenario the permeable fault zone facilitates downward flow, even while facilitating upward flow above the deep clay cap. The downward flow is relatively slow, resulting in negligible temperature change from the base-case. A similar situation occurs when the fault is offset by -1000 m: the uppermost 1550 m of the fault zone facilitates upward flowing fluid, while the lower 450 m facilitates downward flow.

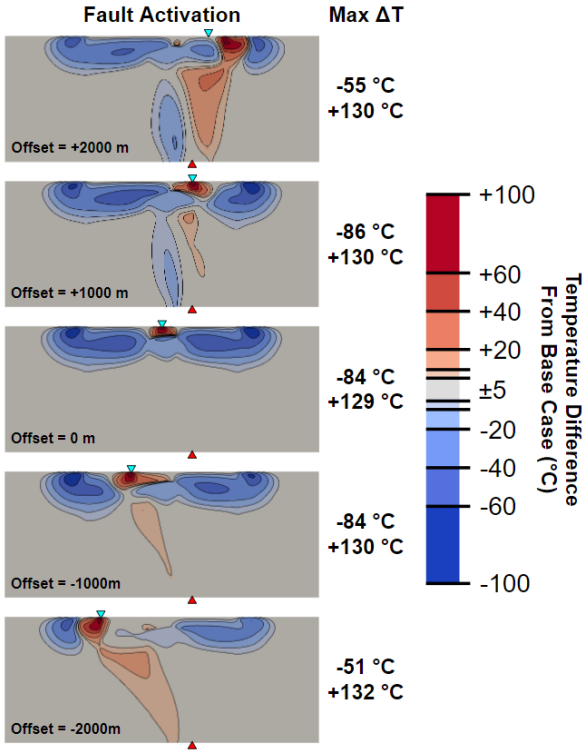

Figure 10: Change in reservoir temperature in response to fault reactivation in a system with a shallow and deep clay cap. Location of the vertical fault zone varies with each model, with varying lateral offset from the model's centreline: 0 m, 500 m, 1000 m, 1500 m, 2000 m, and 2500 m. Colours and contours are set at ±5, ±10, ±20, ±40, ±60, and ±100 °C. Grey represents a temperature difference of less than ±5 °C. Red triangle represents centre line. Turquoise triangle fault location at surface.

5. DISCUSSION

5.1 Changes over time

Both the eruption zone and fault zone result in increased temperature in their immediate vicinity within 500 years. This is due to the flow of hot fluid into and through the area. The physical extent of this heated region changes little with time. Although the magnitude of the temperature change increases over time, most of the heating occurs within the first 500 years.

The hydrothermal eruption is modelled as a zone of increased permeability which is 100 m wide and extends 200 m below the surface, penetrating the shallow clay cap (from 100 to 200 m) but not the deep clay cap (from 800 to 1000 m). This results in temperature changes which are mostly limited to the shallow reservoir above the deep clay cap, but which are nonetheless significant. In the models presented here, temperature changes on the order of ±30 to ±160 °C are observed after 5,000 years. This shows that a hydrothermal eruption is capable of inducing large changes in shallow reservoir temperature, provided the eruption zone remains relatively permeable (i.e., ≥ 1E-15 m^2). However, temperature changes in the deep reservoir constrained by the deep clay cap are minor, with virtually no effect below 2000 m depth. It is only when the deep clay cap becomes permeable or absent that temperature conditions are impacted in the deeper reservoir.

The fault zone is similarly modelled as a zone of higher permeability 20 m wide and extending 2000 m below the surface. Because it penetrates both the shallow and deep clay caps, the temperature changes associated with the fault zone extend deeper into the reservoir. Within 500 years, the rock in the immediate vicinity of the fault zone is heated over +120 °C and increases slightly up to +130 °C at 5,000 years. The cooling effect, however, is not significant until 1,000 years and increases slowly up to 5,000 years, from -49 to -86 °C.

5.2 Varying feature permeability

The models presented here feature constant permeability. When the eruption zone permeability is reduced, the temperature does not decline linearly: permeability greater than or equal to 1E-15 m^2 results in similar temperature changes, but below this the temperature changes quickly reduce. Any reduction in fault zone permeability, however, will reduce both the extent and magnitude of temperature changes. The difference in fault versus eruption zone behaviour may be due to the narrow width of the fault, where the permeability times thickness product is too small to meaningfully impact the reservoir's convection patterns.

5.3 Varying deep clay cap permeability

Increasing clay cap permeability from impermeable (1E-19 m^2) to as permeable as the reservoir (1E-15 m^2) results in diverging temperature changes: heating effects increase and cooling effects weaken. In both the hydrothermal eruption and fault models, temperature increases extend deeper into the reservoir. This is probably because fluid upflow zones are more readily changed without a clay cap, which restricts upflow through a narrow gap in the centre of the model.

The key difference between the hydrothermal eruption zone and fault zone is that the fault zone penetrates the deeper clay cap. As the effect of the flow-restricting clay cap disappears, both features are in hydraulic connection with the deeper reservoir, causing results to converge, resulting in similar temperature changes from the base-case.

5.4 Varying fault zone location

The location of a hydrothermal eruption is limited to regions of near boiling fluids below the shallow clay cap exist. In the models presented here, such conditions are located within a few hundred meters to either side of the model's centreline. By shifting the location of the fault zone within this region, we show that the location of such an event has little impact on the magnitude of temperature increases it induces. All models shown in Figure 10 result in a temperature increase of +130 to +132 °C.

The cooling effects observed, however, appear to decrease when the fault zone is located at the margins of the reservoir. This indicates that hot water from other parts of the reservoir are more likely to be drawn by a fault located near the upflow zone.

5.5 Further works

The topography of the system was modelled as a flat plain in order to simplify the model. Addition of realistic topography would induce shallow aquifer cross flows from high to low topography, altering the temperature field of the base model. Subsequent changes in temperature due to hydrothermal eruptions or fault zones would likely produce similar results, perhaps with slightly different behaviour near the surface.

6. CONCLUSIONS

We have presented numerical reservoir simulations to assess the impact (a) a hydrothermal eruption and (b) a fault on the thermal structure of a geothermal system. These results were compared to a base-case simulation where the geothermal system remained unperturbed. The duration for all three simulations was 5000 years.

The subsequent temperature differences are shown for several varying parameters: time since emplacement, eruption/fault zone permeability, deep clay cap permeability, and eruption/fault zone location. In penetrating the shallow clay cap, both a hydrothermal eruption zone and a fault zone provide a permeable conduit through which hot, upwelling fluid can reach the surface. This results in heating of the nearby rock and cooling on the margins of the reservoir.

These models indicate that a hydrothermal eruption or a fault zone can induce large changes in the temperature field of a geothermal reservoir, including both proximal heating and distal cooling. The changes following a hydrothermal eruption are likely to remain within the shallow reservoir, while changes resulting from fault activation tend to extend deeper in the reservoir.

These results are meant to serve as a reference of the potential effects of a hydrothermal eruption or permeable fault zone over 5,000 years. While large temperature changes are possible in the shallow to intermediate depths of the reservoir, deep changes to upflow convection patterns are only slight. Although the upflow zone at the bottom of the reservoir is fixed in these simulations, the convection patterns in the deeper reservoir remain relatively static, suggesting that such surface events are unlikely to induce significant flow pattern changes below their maximum depth.

ACKNOWLEDGEMENTS

Funding for this project was provided from GNS Sciences Strategic Investment Fund for "New Zealand's Geothermal Future C05X1702".

REFERENCES

Bignall, G., and Browne, P.R.L.: Surface hydrothermal alteration and evolution of the Te Kopia geothermal field, New Zealand: Geothermics, v. 23, p. 645-658. (1994).

Bignall, G., Sekine, K. And Tsuchiya, N.: Fluid-rock interaction processes in the Te Kopia geothermal field (New Zealand) revealed by SEM-Cl imaging. Geothermics, v. 33, p. 615-635. (2004).

Browne, P.R.L., and Lawless, J.V.: Characteristics of hydrothermal eruptions, with examples from New Zealand and elsewhere. Earth Science Reviews. v. 52, p. 299–331. (2001)

Burnell, J., Clearwater, E., Croucher, A., Kissling, W., O'Sullivan, J.P., O'Sullivan, M.J. & Yeh, A.: Future directions in geothermal modelling, Proceedings (electronic) 34rd New Zealand Geothermal Workshop, University of Auckland, Auckland, New Zealand, 19-21 November, 2012. (2012).

Chambefort, I., Buscarlet, E, Wallis, I.C., Sewell, S., and Wilmarth, M.: Ngatamariki Geothermal Field, New Zealand: Geology, geophysics, chemistry and conceptual model: Geothermics, v. 59, p. 266–280. (2016).

Collar, R.J., and Browne, P.R.L.: Hydrothermal eruptions at the Rotokawa Geothermal Field, Taupo Volcanic Zone. In: Proceedings of the 7th New Zealand Geothermal Workshop, University of Auckland, Auckland, New Zealand, p. 171–175. (1985).

Dempsey, D.E., Rowland, J.V., Zyvolosky, G.A., Archer, R.A.: Modeling the effects of silica deposition and fault rupture on natural geothermal systems. J. of Geophys. Research, v. 117 (2012).

Heap, M.J. et al.: A multidisciplinary approach to quantify the permeability of the Whakaari/White Island volcanic hydrothermal system (Taupo Volcanic Zone, New Zealand). *Journal of Volcanology and Geothermal Research,* v. 332, p.8 88-108. (2017).

Montanaro, C., Cronin, S.J., Lerner, G., Simpson, M.P., Brooks-Clarke, I., Swanney, G., Milicich, S.D., Calibugan, A., Bardsley, C., Scheu, B.: Natural processes leading to large, pre-histpric hydrothermal eruptions n geothermal areas: Rotokawa geothermal field, New Zealand: GSA Bulletin - Geological Society of America. (2023).

O'Brien, J.M., Mroczek, E., and Boseley, C.: Chemical structure of the Ngatamariki geothermal field, Taupo Volcanic Zone, New Zealand. Proceedings of the 35th New Zealand Geothermal Workshop, Auckland, New Zealand. (2011).

Pruess, K., Oldenburg, C., and Moridis, G.: TOUGH2 User's Guide, Version 2.0. Berkeley: Earth Sciences Division, Lawrence Berkeley National Laboratory. (1999).

Sewell, S.M., Addison, S.J., Hernandez, D., Azwar, L., and Barnes, M.L.: Rotokawa conceptual model update 5 years after commissioning of the 138 MWe NAP Plant. In: Proceedings of the 37th New Zealand Geothermal Workshop, Taupo, New Zealand, paper 098. (2015).

Simmons, S.F., Keywood, M., Scott, B.J., Keam, R.F.: Irreversible change of the Rotomahana–Waimangu hydrothermal system (New Zealand) as a consequence of a volcanic eruption: Geology, v. 21, p. 643–646. (1993).

Simmons, S.F., O'Sullivan, M.: Numerical Model of the Changes in Geothermal Activity in the Rotomahana-Waimangu System Due to the 1886 Eruption of Mt Tarawera. Proceedings World Geothermal Congress 2010, Bali, Indonesia (2010).

Simpson, M.P., Morales, A.G., Chambefort, I., Alcaraz, S., Moribe, S., Milicich, S.D., Calibugan, A., Grove, T., and Zealand, N.: Hydrothermal minerals and hydrologic evolution of the Rotokawa geothermal system, New Zealand, in Proceedings of the 43rd New Zealand Geothermal Workshop, University of Auckland, Auckland, New Zealand. (2021).

Tontini, F.C., de Ronde, C., Scott, B., Soengkono, S., Stagpoole, V., Timm, C., Tivey, M.: Interpretation of gravity and magnetic anomalies at Lake Rotomahana: geological and hydrothermal implications. Journal of Volcanology and Geothermal Research. (2015).

Winick, J., Powell, T., and Mroczek, E.: The natural-state geochemistry of the Rotokawa reservoir. In: Proceedings of the 33rd New Zealand Geothermal Workshop, University of Auckland, Auckland, New Zealand, 8p. (2011).

ISSN 2703-4275